Influence of the Madden-Julian Oscillation on moisture transport by the Caribbean Low Level Jet during the Midsummer Drought in Mexico

Juliet Perdigón-Morales[a], Rosario Romero-Centeno[a,*], Paulina Ordoñez[a], Raquel Nieto[b], Luis Gimeno[b], Bradford S. Barrett[c]

[a] *Centro de Ciencias de la Atmósfera, Universidad Nacional Autónoma de México, Mexico City, Mexico*
[b] *Environmental Physics LABoratory (EPhysLab), CIM-UVIGO, University of Vigo, Ourense, Spain*
[c] *Oceanography Department, U.S. Naval Academy, Annapolis, Maryland, USA*

ARTICLE INFO

ABSTRACT

This study aims to improve the understanding of the role of the Madden-Julian Oscillation (MJO) in modulating the midsummer drought (MSD) in Mexico. First, the main moisture sources for the MSD region in Mexico during the summer were identified using the Lagrangian particle dispersion model FLEXPART for the period 1979–2017. From this analysis, the Caribbean Sea was identified as one of the main moisture sources, particularly the area where the core of the Caribbean low-level jet (CLLJ) is located. Second, the water vapour flux transported by the CLLJ to Mexico was then analysed. It was found that the summer seasonal cycle of the CLLJ is associated with the bimodal precipitation pattern in Mexico through the seasonal variability of the moisture contribution from the CLLJ to precipitation over the MSD region, thereby confirming the CLLJ as a key element in the occurrence of the MSD in the Americas. Third, the influence of the MJO on this transport was examined. This analysis showed that the locally dry phases of the MJO decrease the contribution of moisture from the CLLJ core towards the MSD region, while the locally wet phases increase it. Moreover, phases 1 and 2 of the MJO were found to influence the first precipitation peak that occurs in the southwestern region of Mexico by increasing the contribution of moisture from the northeastern tropical Pacific. The study ends by proposing, for the first time, a mechanism by which the MJO modulates the MSD in Mexico.

1. Introduction

The annual cycle of precipitation in the Pacific coast of Central America, the Caribbean, and the central, southern, and some regions of northern Mexico exhibits a bimodal behaviour, with precipitation maxima at the beginning and end of the rainfall season and a relative minimum in between (e.g. Magaña et al., 1999; Curtis, 2002; Amador et al., 2006; Small et al., 2007; Gamble et al., 2008; Karnauskas et al., 2013; Perdigón-Morales et al., 2018). This relative minimum in precipitation, which generally occurs during July–August, is known as the midsummer drought (MSD; Magaña et al., 1999).

The physical forcing mechanisms associated with this precipitation pattern include the variability of the position and strength of the intertropical convergence zone (ITCZ) and of the North Atlantic subtropical high pressure system (e.g. Giannini et al., 2000; Mapes et al., 2005; Romero-Centeno et al., 2007; Small et al., 2007; Gamble et al., 2008), and the intensification of the Caribbean low-level jet (CLLJ;

Amador, 1998; Amador et al., 2000; Whyte et al., 2008) and associated direct circulations and sea surface temperature variability (e.g. Magaña and Caetano, 2005; Herrera et al., 2015). The latter is the mechanism that has greatest consensus in the scientific community as explaining the MSD (e.g. Wang, 2007; Gamble and Curtis, 2008; Muñoz et al., 2008; Cook and Vizy, 2010; Martin and Schumacher, 2011b; Hidalgo et al., 2015; Maldonado et al., 2016). All of these processes interact with, and are likely modulated by, larger-scale modes of atmospheric and oceanic variability (Perdigón-Morales et al., 2019). Indeed, several recent studies have suggested that the Madden-Julian Oscillation (MJO) may influence the physical mechanisms behind the MSD (e.g. Martin and Schumacher, 2011a; Curtis and Gamble, 2016; Perdigón-Morales et al., 2019).

The MJO is the dominant mode of tropical intraseasonal variability, and it is characterised by a large-scale coupled pattern of atmospheric circulation and deep convection propagating eastward from the Indian Ocean along the equator with a period of 30–60 days (Madden and

---

Julian, 1994; Hendon and Salby, 1994). The MJO has significant effects on atmospheric circulation throughout the global tropics. In the Western Hemisphere specifically, the MJO has been shown to modulate the intraseasonal variability of rainfall in the Americas and the Caribbean (e.g. Lorenz and Hartmann, 2006; Barlow and Salstein, 2006; Martin and Schumacher, 2011a; Zhou et al., 2012; Barrett and Esquivel, 2013; Curtis and Gamble, 2016; Perdigón-Morales et al., 2019), the intraseasonal variability of sea surface temperature and the low-level winds and surface fluxes in the northeastern tropical Pacific (NETP) (e.g. Higgins and Shi, 2001; Maloney and Kiehl, 2002; Maloney and Esbensen, 2003, 2007; Lorenz and Hartmann, 2006; Maloney et al., 2008), and the hurricane activity in the eastern Pacific (e.g. Maloney and Hartmann, 2000a; Crosbie and Serra, 2014) and North Atlantic oceans (e.g. Maloney and Hartmann, 2000b; Barrett and Leslie, 2009; Klotzbach, 2010). In general, the westerly low-level zonal wind anomalies associated with the active phase of the MJO favour periods of enhanced low-level moisture convergence, surface latent heat fluxes, and organized convection in the NETP, as well as the development of hurricanes in this basin. These processes, in turn, have an important influence on the continental rainfall (e.g. Maloney and Esbensen, 2003, 2007; Lorenz and Hartmann, 2006). Conversely, the easterly low-level wind anomalies associated with the suppressed phase of the MJO lead to large-scale subsidence and drying of the lower atmosphere, suppressing convection and hurricane activity in the NETP.

Furthermore, the MJO has been shown to modulate the MSD in the Americas (e.g. Curtis and Gamble, 2016; Zhao et al., 2019; Perdigón-Morales et al., 2019). For example, Curtis and Gamble (2016) found that a strong MJO signal over the Maritime Continent in winter can lead to a positive North Atlantic Oscillation in March, a pressure pattern that then produces accelerated trade winds within the Caribbean Sea at the beginning of summer. These winds evaporatively cool the sea surface and lead to a reduction of convection and precipitation in the Caribbean, southern Mexico, and the eastern Pacific. Perdigón-Morales et al. (2019) (hereafter PM19) found that the MJO phases related with the least precipitation in Mexico during summer (4, 5, and 6; hereafter referred to as the locally "dry phases") are the most frequent during the MSD minimum, whilst those related with more precipitation (8, 1, and 2; hereafter referred to as the locally "wet phases") are the most frequent during the second rainfall peak. These results indicate that the MJO influences the bimodal pattern of precipitation in Mexico by inhibiting convection and precipitation during the MSD minimum and favouring them during the second rainfall peak. However, there are still knowledge gaps regarding the possible physical mechanisms and moisture source regions that may link MJO to MSD in Mexico.

The identification of water vapour sources for precipitation, and the mechanism for atmospheric moisture transport from these sources, become important issues by which we understand the variability of precipitation in a region (e.g. Brubaker et al., 1993; Trenberth, 1999). The origin of moisture in Mexico, particularly for the western North American monsoon (WNAM) region, has been widely studied (e.g. Mitchell et al., 2002; Bosilovich et al., 2003; Ordoñez et al., 2019). Low-level moisture from the eastern tropical Pacific and the Gulf of California and mid-level water vapour from the Caribbean Sea and the Gulf of Mexico have been identified as important sources of moisture for the WNAM system (e.g. Mitchell et al., 2002; Ordoñez et al., 2019). Local continental evaporation has also been recognised as an important source of moisture for monsoon precipitation in North America (e.g. Bosilovich et al., 2003; Ordoñez et al., 2019). Likewise, the Gulf of Mexico and the Caribbean basin, the Gulf of California, and northwestern Mexico have been identified as major moisture sources for northern Mexico (Nieto et al., 2014). Moreover, Durán-Quesada et al. (2010) studied an area that includes the Yucatan Peninsula in their analysis for Central America and found the Caribbean Sea to be the main moisture source for that region. However, as far as we know, the moisture sources for the principal MSD region of Mexico have not previously been investigated, at least not through Lagrangian methods.

More generally, several studies have shown the importance of the Caribbean Sea as the main moisture source for rainfall over the Gulf of Mexico and the continental United States (e.g. Mestas-Nuñez et al., 2007; Cook and Vizy, 2010; Nieto et al., 2014), and many studies have confirmed the relevance of the CLLJ as a main regional moisture conveyor (e.g. Cook and Vizy, 2010; Durán-Quesada et al., 2010, 2012, 2017).

The CLLJ is an easterly wind jet with a core located at the 925 mb level over the Caribbean Sea (~12.5°N - 17.5°N, 70°W - 80°W), between northern South America and the Greater Antilles. The CLLJ is present throughout the year and has two maxima, in February and July, and two minima, in May and October (Wang, 2007). The dynamics and temporal variability of the CLLJ plays an essential role in the occurrence of the MSD in the Caribbean (e.g. Wang, 2007; Gamble and Curtis, 2008; Muñoz et al., 2008; Cook and Vizy, 2010; Martin and Schumacher, 2011b), Central America and the NETP (Magaña and Caetano, 2005; Herrera et al., 2015; Hidalgo et al., 2015; Maldonado et al., 2016). The intensification of the CLLJ during July is associated with an increase in evaporation over the Intra-Americas Sea, which increases the humidity over the ocean available for export (Cook and Vizy, 2010). The maximum low-level moisture convergence in the CLLJ exit region increases vertical latent heat flux and reduces atmospheric stability, supporting the maximum in tropical convection over the Caribbean coast of Central America. This intense convection in the western Caribbean Sea plays an important role in modulating convective activity in the surrounding regions through a zonally direct circulation, imposing subsidence and inhibiting convection in those surrounding regions (e.g. Magaña and Caetano, 2005; Whyte et al., 2008; Gamble and Curtis, 2008; Herrera et al., 2015; Hidalgo et al., 2015). Additionally, this CLLJ-associated regional atmospheric circulation leads to a southward displacement of the ITCZ in the NETP in July–August, thus influencing the rainfall pattern on the Pacific regions by generating changes in local moisture sources (Hidalgo et al., 2015). Moreover, the strengthening of the CLLJ intensifies the gap flow over Central America that reaches the NETP. The strong low-level easterly winds, in addition to lowering sea-surface temperatures, produce a westward shift in low-level moisture convergence. This westward shift in moisture convergence, combined with subsidence, results in the MSD over the tropical Americas (e.g. Herrera et al., 2015).

While the role of the CLLJ in the occurrence of the MSD has been widely demonstrated for the tropical Americas (e.g. Wang, 2007; Whyte et al., 2008; Herrera et al., 2015), none of the studies has considered the entire region where MSD occurs in Mexico (with the exception of southern Mexico), even though it is well known that the bimodal pattern extends more to the north (e.g. Curtis, 2002; Karnauskas et al., 2013; Perdigón-Morales et al., 2018). Moreover, the MJO also modulates the CLLJ (e.g. Martin and Schumacher, 2011a; Curtis and Gamble, 2016; García-Martínez and Bollasina, 2020). The CLLJ varies significantly between phases of the MJO: westerly surface wind anomalies during MJO phases 1 and 2 (when the MJO convection is passing over the Western Hemisphere, Africa, and the western Indian Ocean) act to slow down the CLLJ, while anomalous surface easterlies in MJO phases 5 and 6 (when the MJO convection is passing from the Maritime Continent into the western Pacific Ocean) act to increase it (Martin and Schumacher, 2011a). Although the MJO modulates both the CLLJ and the MSD in Mexico, the possible combined MJO-CLLJ action on the MSD in Mexico has not been studied before.

To better understand the mechanism by which the MJO modulates the MSD over Mexico, this study investigates the possible influence of the MJO on moisture transport towards the MSD region in Mexico. A valuable tool for the identification of moisture sources and for the assessment of moisture source-sink relationship is the Lagrangian method (e.g. Gimeno et al., 2012). In this sense, the Lagrangian approach has been extensively applied to analyse the role of synoptic-scale systems such as low-level jets, atmospheric rivers, and monsoons on precipitation over continental areas all around the globe (e.g. Algarra et al.,

2019; Ramos et al., 2016; Ordoñez et al., 2019), as well as for analyzing the role of moisture sources in the diagnosis of the occurrence of extreme hydroclimatic events (drought and heavy precipitation events) (see Gimeno et al., 2020, a recent review). However, to the best of the authors' knowledge, studies focused on the analysis of moisture transport towards Mexico from a Lagrangian point of view are scarce for the MSD region. Moreover, although the occurrence of the MSD in the tropical Americas has been associated with the CLLJ, none of the studies has shown a CLLJ-MSD modulation by the MJO. To achieve this, the study focuses on the following: (1) the identification of the major climatological moisture sources for the MSD region in Mexico; (2) the evaluation of the role the moisture transport towards Mexico plays on the bimodal precipitation pattern, and (3) the analysis of the influence of the MJO on moisture transport to the MSD region in Mexico. The study concludes by proposing a mechanism by which the MJO modulates the MSD in Mexico.

The next section provides a description of the data, the MJO index, and the analysis methodology. The results of the study are presented and discussed in section 3, and section 4 provides a summary and conclusions.

2. Data and analysis procedures

In this study, the atmospheric water vapour transport towards the MSD region in Mexico is investigated using a three-dimensional Lagrangian particle dispersion model (FLEXPART v9.0; Stohl and James, 2005) and the methodology of Stohl and James (2004, 2005). FLEXPART has shown coherent results at the regional and global scales for climatological assessment of oceanic and continental moisture source regions (e.g. Gimeno et al., 2012, 2013), and here it is applied to Mexico. Moreover, the Lagrangian approach to water vapour transport based on FLEXPART has shown compatible results to those obtained using an Eulerian method (e.g. Stohl and James, 2005; Ordoñez et al., 2019). A Lagrangian technique was used in this work since (1) is more suitable for climatological analysis (Gimeno et al., 2020), and (2) it allows forward and backward tracking of particles along their trajectories, determining the source-receptor water vapour relationships (e.g. Gimeno et al., 2012). Changes in the specific humidity along the trajectory of each particle that link the moisture source with moisture sink regions were calculated using FLEXPART driven by gridded meteorological data from the ERA-Interim reanalysis (Dee et al., 2011) of the European Centre for Medium-Range Weather Forecasts (ECMWF) for May–October from 1979 to 2017. The ERA-Interim reanalysis is available with a horizontal resolution of $1° \times 1°$ and 61 vertical levels. Analyses from every 6 h (00:00, 06:00, 12:00, and 18:00 UTC) and 3 h forecasts at intermediate times (03:00, 09:00, 15:00, and 21:00 UTC) were used. The latter were needed to complement the calculations with FLEXPART because the higher time resolution is critical for the accuracy of Lagrangian trajectories (Stohl et al., 1995).

The water vapour flux is calculated in FLEXPART as follows. Initially, the atmosphere is homogeneously divided into a large number of air particles, each representing a fraction of the total atmospheric mass. These particles are advected by a 3-D wind field, considering parameterizations for turbulence and convection, and with their mass (m) kept constant. The specific humidity (q) and the position (latitude, longitude, and altitude) of each air particle are recorded at 6-h intervals. Then, the net rate of change in water vapour content (e - p) at each time step and for each air parcel is computed from the temporal derivative of specific humidity:

$$e - p = m \frac{dq}{dt}$$

(1)

where e and p are the rates of moisture increase and decrease of the particle along the trajectory, respectively. To estimate the net surface water flux ($E - P$) in an area A, the moisture change of all parcels in the atmospheric column over A is considered as follows:

$$E - P = \frac{\sum_{k=1}^{K} (e - p)}{A}$$

(2)

where K is the number of particles over the area A and E and P are the rates of evaporation and precipitation per unit area, respectively.

The air particles can be followed both backwards and forwards in time, and the gain and loss of moisture along their trajectories as they leave and arrive into a target area can be identified. The mean residence time of the water vapour in the atmosphere is estimated to be about 8–10 days over Mexico and the Intra-Americas Sea (see Fig. 2 in Van Der Ent and Tuinenburg, 2017). Moreover, Nieto and Gimeno (2019) identified the optimal time of integration for Lagrangian studies and found values very similar to those defined by Van Der Ent and Tuinenburg (2017). A travel time of 10 days is therefore used in this work to determine the climatological moisture sources and sinks related to a region. Hereafter, $(E - P)_n$ indicates the net moisture balance for day "n", where n varies from day 1 to day 10 after the particles begin to move. The sum of $(E - P)_1$ to $(E - P)_n$ is indicated as $(E - P)_{1-n}$ and is a measure of the mean gain or loss of moisture in the atmosphere between day 1 and day n after the particles departed the target region.

The $(E - P)_{1-10}$ field integrated over backward trajectories indicates a moisture source region for a target area when $E - P > 0$, while the $(E - P)_{1-10}$ field integrated over forward trajectories shows a moisture sink region for a target area when $E - P < 0$. Both backward and forward trajectories were used in this work. Because the analysis period is long (39 years), this method can identify the regions that are sources and sinks of moisture from a climatological perspective. The limitations and uncertainty of this Lagrangian approach, and its advantages and disadvantages with respect to other methods that estimate moisture sources, are discussed in Gimeno et al. (2012) and, more recently, Ordoñez et al. (2019).

The vertically integrated atmospheric moisture flux (VIMF) provides an approximation of the moisture transport in the atmosphere. The divergence of the VIMF is in equilibrium with the difference between evaporation and precipitation, giving an estimation of the moisture flux balance (Stohl and James, 2004). The VIMF, along with the FLEXPART calculations of the water vapour flux (E - P), were used to analyse how the MJO modulates the moisture transport over Mexico. For this purpose, the ERA-Interim 6-hourly (00:00, 06:00, 12:00, 18:00 UTC) gridded components of the vertically integrated eastward and northward water vapour fluxes, and the divergence of the VIMF, were analysed from May to October for the period 1979–2017. Those values were used to calculate daily averages and, in this case, the spatial resolution of these gridded products was $0.75° \times 0.75°$.

Anomaly composites were used to analyse the temporal and spatial variability of $E - P$, the VIMF, and the divergence of VIMF as a function of the MJO phase. The daily magnitude (amplitude) and geographic location (phase) of the MJO were determined using the Real-time Multivariate MJO index (RMM; Wheeler and Hendon, 2004). Only active MJO days, which are those with an index amplitude greater than 1.0 (Wheeler and Hendon, 2004), were considered in this study. The index includes eight phases, each of which provides an approximate location of the MJO active phase as it propagates eastward from the Indian Ocean (Wheeler and Hendon, 2004). A composite was generated for each active phase of the MJO and for each month of the rainy season (from May to October). The Monte Carlo technique was applied to test the statistical significance of all MJO composites with ten thousand iterations, following Efron and Tibshirani (1994).

3. Results and discussion

3.1. Climatological moisture sources of the MSD region in Mexico

Backward Lagrangian trajectories were used to identify the main moisture sources for four regions in Mexico, which are shown in Fig. 1. These four regions were chosen based on the areas where different
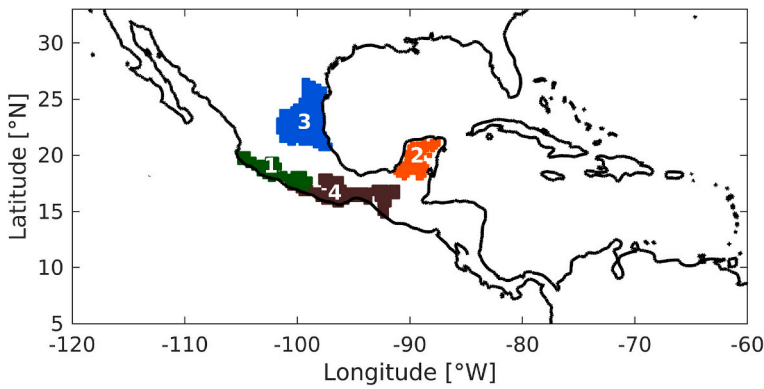
Fig. 1. Regions representing different types of MSD in Mexico according to Perdigón-Morales et al. (2018): (1) the southwest region for the August-only MSD, (2) the Yucatan Peninsula for the July-only MSD, (3) the south and (4) northeast regions for the July–August MSD. These regions were used for the backward analysis with FLEXPART.

types of MSD occur in Mexico, according to Perdigón-Morales et al. (2018): (1) the southwestern region that encloses a portion of the area with August-only MSD; (2) the region in the Yucatan Peninsula that contains a portion of the area with July-only MSD, and (3) the northeastern and (4) southern regions which include portions of the area with July–August MSD. Fig. 2 shows the monthly climatologies, from
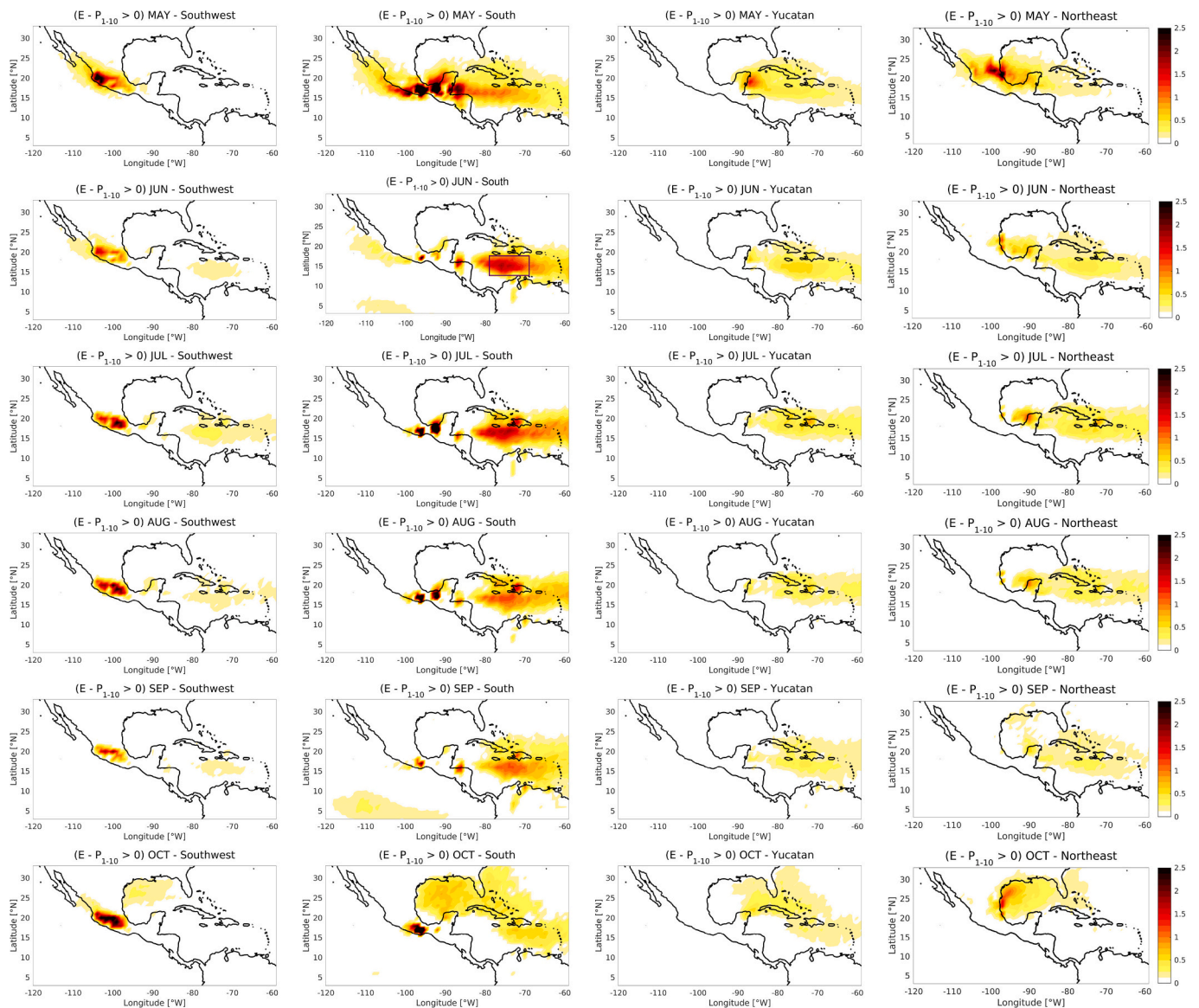
Fig. 2. Monthly climatological values of $(E − P)$ (mm day^{-1}) integrated backwards for 10 days [$(E - P)_{1–10}$] starting from the four MSD subregions in Mexico (from left to right): southwest, south, Yucatan Peninsula, and northeast. The results are shown from May (top panels) to October (bottom panels) for the period 1979–2017. Only the grid points exceeding the 95th percentile of $(E − P)_{1–10} > 0$ are displayed, which represent evaporative regions or moisture sources. The rectangle shown on the June map for the south region corresponds to the CLLJ core area (~12.5°N-17.5°N, 70°W-80°W), which was used for the forward analysis with FLEXPART.

May to October, of the water vapour flux integrated backwards from these four subregions for 10 days [$(E − P)_{1−10}$ from now on]. In order to identify the most important moisture source regions, only the grid points with values that exceed the 95th percentile of $(E − P)_{1−10} > 0$ are analysed and shown in Fig. 2.

The Lagrangian approach highlights differences between the subregions where MSD occurs. While in general the Caribbean Sea emerges as a moisture source for all of them, mainly from June to September (Fig. 2), the Gulf of Mexico also emerges as an important source, mainly for northeastern and southern Mexico in May and October when the moisture contribution from the Caribbean reaches its minimum. The contribution of moisture from the Caribbean is more important for the southern region and less for the southwestern region. There is a clear seasonal variability in both the intensity and the horizontal extent of the evaporative area in the Caribbean during summer, with relatively high values in June–July when it contributes humidity for the four subregions, and with low values in October when it contributes humidity only for southern Mexico and the Yucatan Peninsula. For northeastern Mexico and the Yucatan Peninsula, the moisture source in the Caribbean Sea appears as a zonally elongated area from June to August that shifts northward in July–August.

The southwestern region of Mexico seems to be the most important moisture source for itself throughout the summer, while the moisture over the Yucatan Peninsula and the northeastern region is only important at the beginning and end of the rainy season (Fig. 2). Finally, the Yucatan Peninsula was identified as a permanent moisture source for northeastern and southern Mexico, although with less intensity in the latter. It is interesting to note that the NETP appears as a climatological moisture source only for the southwestern and southern regions in May and June, when an area close to the Mexican coasts is identified as a moisture source, and in June and September for the southern region when an area of the tropical Pacific is identified as a moisture source.

In summary, the results presented in this section show the important role of the Caribbean Sea as a moisture supplier for the MSD region in Mexico during most of the rainy season (mainly from June to September). Despite its seasonal variability, the region with the maximum contribution of moisture over the Caribbean Sea generally coincides with the CLLJ core region (12.5° N – 17.5° N, 70° W – 80° W), in agreement with previous works (e.g. Wang, 2007; Durán-Quesada et al., 2010). Based on this, in the next subsection, the role of the CLLJ as a humidity carrier to the MSD region in Mexico is analysed by determining the corresponding moisture sinks.

3.2. Water budget transported by the CLLJ

Forward Lagrangian trajectories were analysed to track the water vapour flux transported by the CLLJ, allowing the identification of the main moisture sinks over Mexico, $(E − P)_{1−10} < 0$, associated with this source region (box in Fig. 2). The monthly climatologies of the water vapour flux integrated over 10-days after air masses leave the CLLJ core region, from May to October for the period 1979 to 2017 were then analysed (Fig. 3). In May and June, the contribution from the CLLJ area to precipitation over Mexico covers almost the entire MSD region, with the exception of the Yucatan Peninsula in June. The precipitation associated with the transported moisture from the CLLJ core reaches its maximum value in some areas over southern and northeastern Mexico. In July and August, the moisture sink region over Mexico presents a remarkable westward shift compared to the previous two months (Fig. 3). Consequently, the humidity contribution from the CLLJ core to precipitation over the MSD region in Mexico is lower in July and August (the exception being some areas in the center and southwest of Mexico). In September, the sink regions extend eastwards over Mexico, again covering almost the entire MSD region, the Gulf of Mexico and the western Caribbean. In October, the main moisture sink related to the CLLJ core lies further east, covering the western Caribbean Sea, and the moisture contribution from the CLLJ core to the MSD region is very low.

In order to quantify the water budget over Mexico associated with the CLLJ core region, spatial averages of $(E − P)_{1−10}$ from the forward
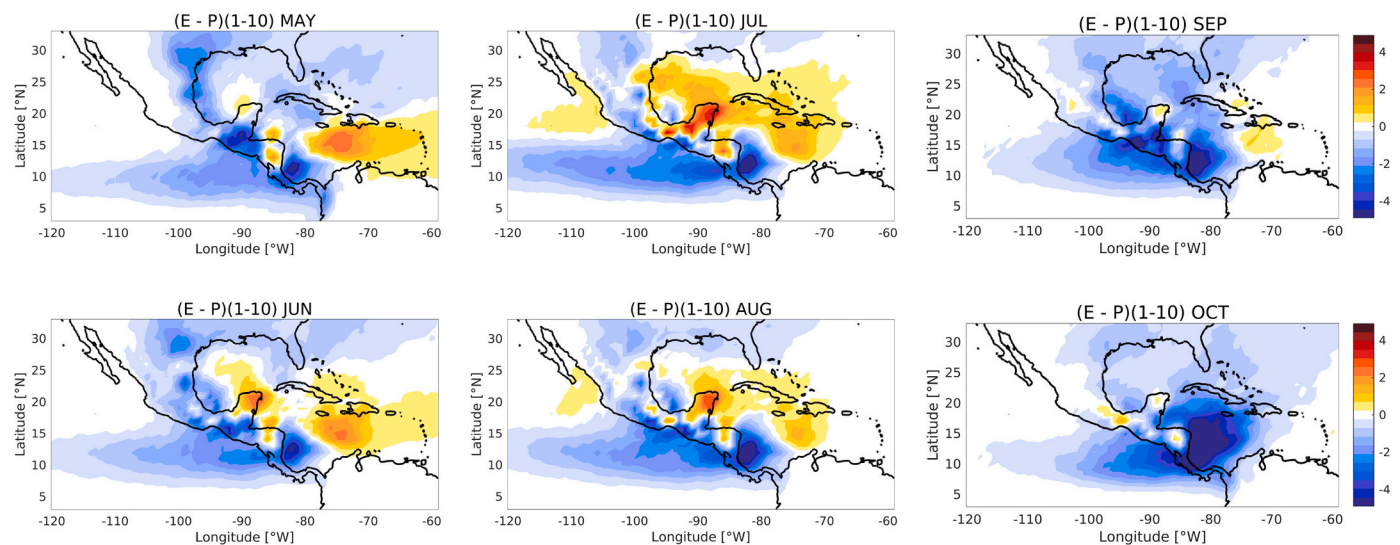

Fig. 3. Monthly climatological values of $(E − P)$ (mm day^{-1}) integrated forwards for 10 days from the CLLJ region from May to October for the period 1979–2017. Negative values represent moisture sinks.
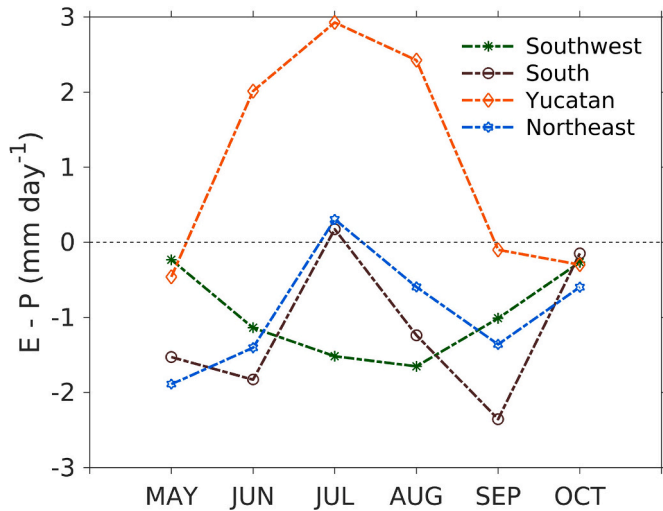
Fig. 4. Seasonal cycle of the water budget $[(E - P)_{1-10}$ (mm day^{-1})] over the four MSD subregions in Mexico (see Fig. 1 for location) associated with the CLLJ core region, from May to October for the period 1979–2017.

analysis over each of the four MSD subregions in Mexico (see Fig. 1) were computed for each month (Fig. 4). The seasonal cycles of $(E - P)_{1-10}$ for the southern and northeastern regions, which feature a July–August MSD, show negative values (predominance of precipitation) throughout the summer, except in July when evaporation dominates. In August, although the seasonal cycle shows negative values in both regions, the water budget is still lower compared to June and September, when the respective first and second rainfall peaks of the season occur. The Yucatan Peninsula, which features a July-only MSD, presents a climatological evaporation dominance of moisture coming from the

CLLJ core region from June to August; however, a peak in evaporation is observed in July, when the MSD minimum occurs in this region. Finally, for the southwestern region of Mexico the $(E - P)_{1-10}$ monthly series shows negative values from May to October. This region features an August-only MSD, and it is in August when the contribution from the CLLJ core to precipitation over this region is greater. These results indicate that the CLLJ does not influence the occurrence of the MSD minimum in the southwestern region as it does in the other three subregions. This implies that other physical mechanisms influence the bimodal rainfall pattern in southwestern Mexico, in agreement with the idea that some processes involved in the occurrence of the MSD on the Pacific side are different from those on the Caribbean (e.g. Herrera et al., 2015; Hidalgo et al., 2015; Maldonado et al., 2016). An analysis for the southwest region of Mexico is presented in section 3.4.

The results presented so far show both the importance of the Caribbean Sea as a moisture source for Mexico and the key role of the CLLJ in the occurrence of the MSD in Mexico. As mentioned in the introduction, MJO modulates both the CLLJ (e.g. Martin and Schumacher, 2011a; Curtis and Gamble, 2016; García-Martínez and Bollasina, 2020) and the MSD (e.g. Curtis and Gamble, 2016; Zhao et al., 2019; PM19). However, until now, the possible combined influence of the MJO-CLLJ on the MSD in Mexico has not been explored. Therefore, the influence of the MJO on the moisture transported towards Mexico by the CLLJ is investigated next.

3.3. Moisture transported by the CLLJ and the propagation of the MJO

Air parcels advected from the CLLJ core area typically begin to precipitate over the MSD region of Mexico three days after leaving that area (Fig. 5). Additionally, for a typical MJO event, phases are separated in time by approximately 5–10 days (Jones and Carvalho, 2011). Since the MJO is in a particular phase each day, using a narrow temporal window (such as 5–6 days) facilitates a clear characterisation of
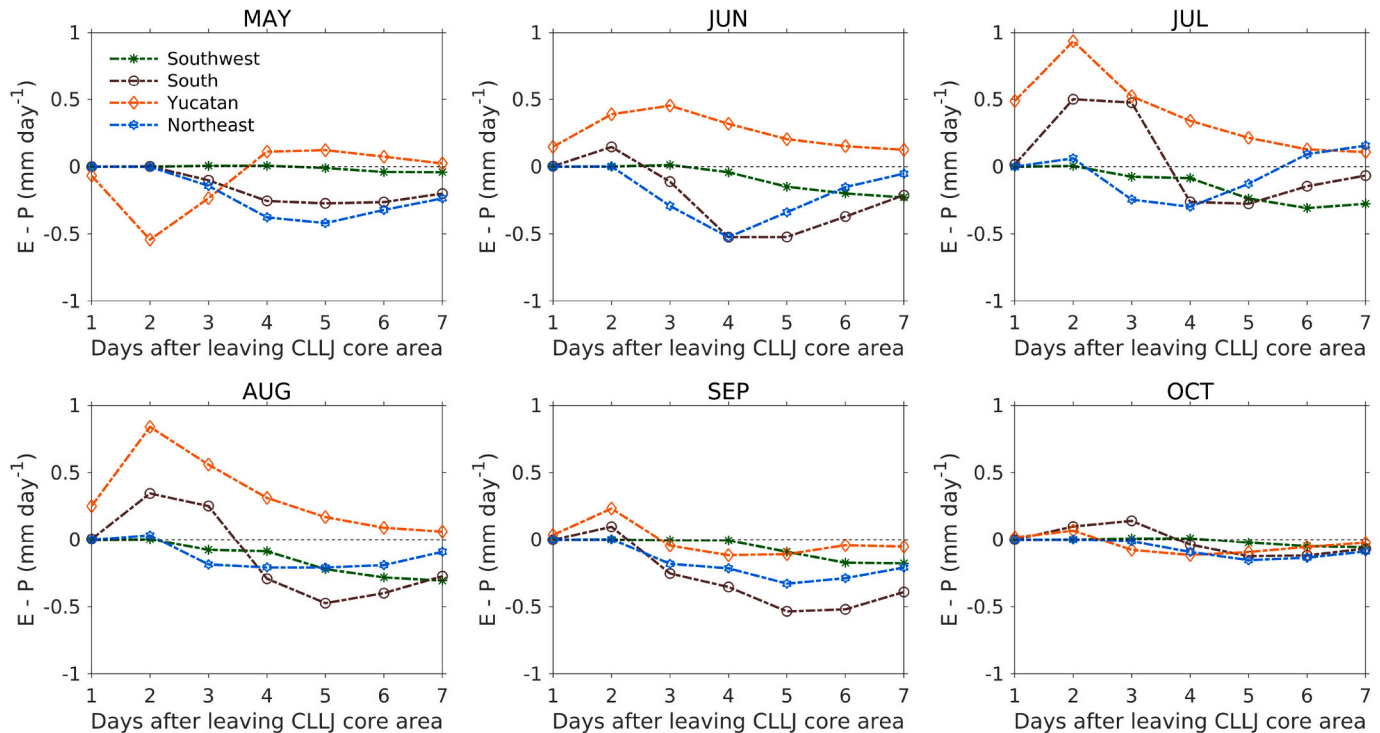

Fig. 5. Monthly time series of $(E - P)_n$ ($n = 1$ to 7) integrated over the four MSD subregions in Mexico associated with the CLLJ core region, from May to October for the period 1979–2017.

the water transport variability related to the MJO, contrary to a wide temporal window (such as 10 days). For these reasons, the temporal range of the trajectories was thus limited to the smallest possible average window of 3–7 days. The $(E − P)_{3−7}$ anomalies, representative of the net water vapour changes for each of the MJO phases, were calculated by matching the last day of the interval (day 7) with every

active MJO day, following Ordonez et al. (2013).

Monthly anomaly composites of the absolute values of $(E − P)_{3−7} < 0$, i.e. $| (E − P)_{3−7} < 0 |$, obtained via forward-in-time trajectories from the CLLJ core (see Fig. 3), were analysed binning by MJO wet phases (Fig. 6) and dry phases (Fig. 7) for each of the summer months (from May to October). Only negative values of $(E − P)_{3−7}$ were
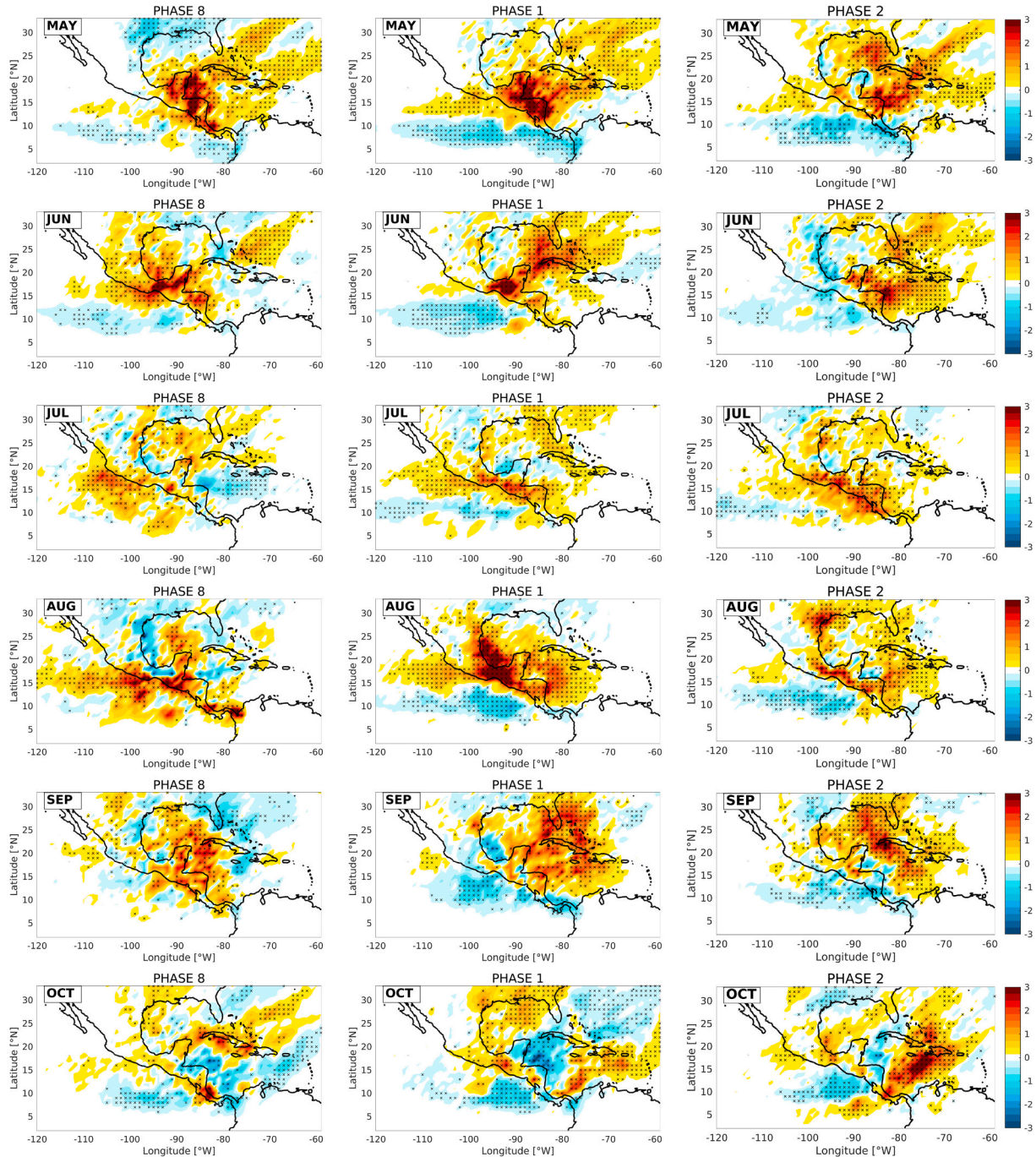
Fig. 6. Anomaly composites of $|(E − P) < 0|$ values (shaded, mm day^{-1}) integrated forwards over 3–7 days from the CLLJ region binned by MJO wet phases (8, 1, 2) from May (top panels) to October (bottom panels). The statistically significant anomalies at the 95% confidence level are indicated with crosses.
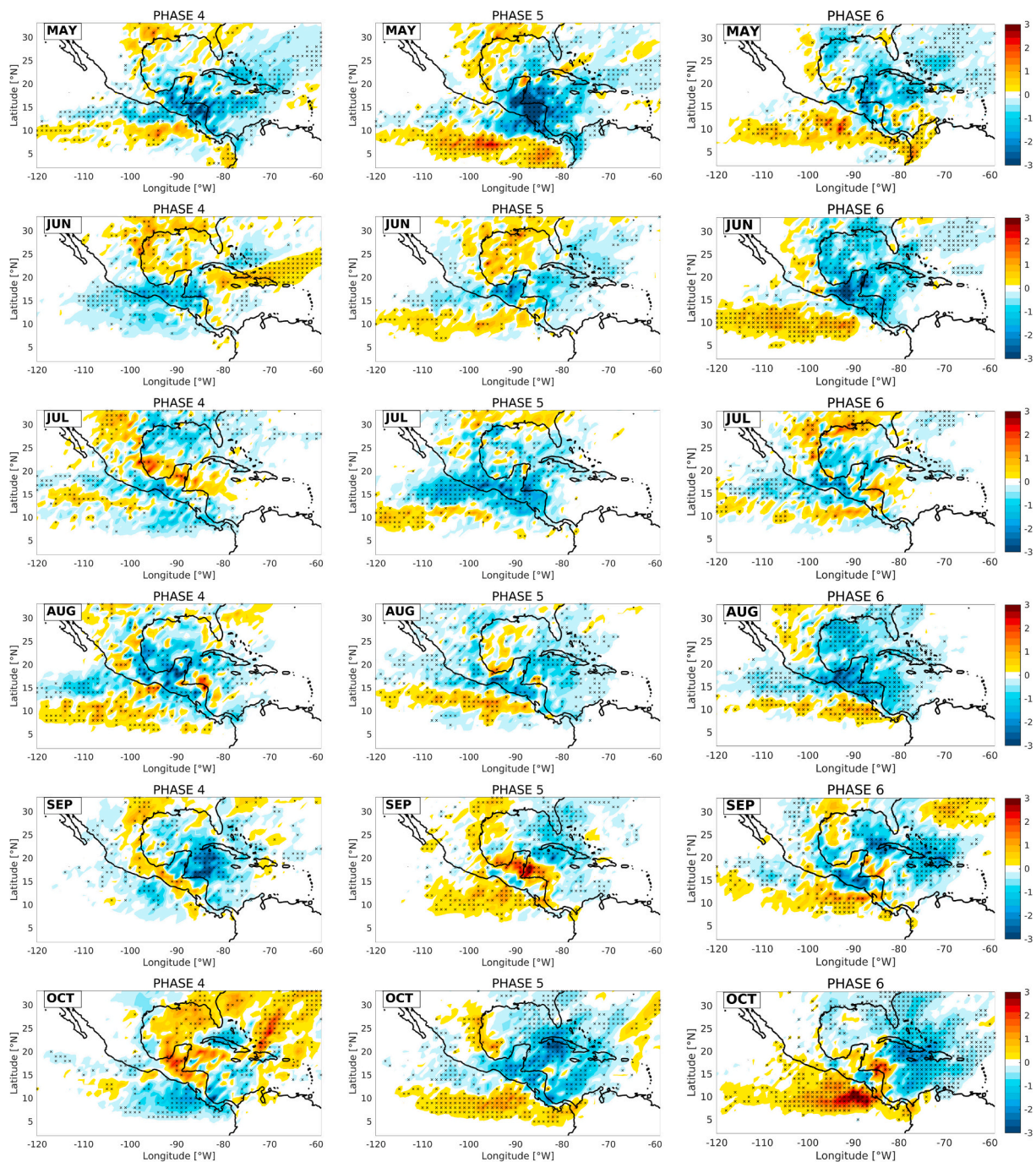
Fig. 7. As in Fig. 6, but for MJO dry phases (4, 5, 6).

used to calculate the anomalies in order to examine how the MJO modulates the moisture sink regions over Mexico associated with the moisture from the Caribbean. Also, monthly anomaly composites of the VIMF and its divergence were created by binning those values by MJO wet phases (Fig. 8) and dry phases (Fig. 9) from June to August (the months when the MSD minimum can occur in Mexico according to PM19).

Although the patterns exhibit regional and temporal variability, in general, MJO wet phases (8, 1, and 2) favour an increase of the

moisture contribution from the CLLJ core region to precipitation mainly over southern Mexico and the Yucatan Peninsula (Fig. 6), while dry phases (4, 5, and 6) inhibit it (Fig. 7). It is worth remembering that positive rainfall anomalies over Mexico and its Pacific and Gulf of Mexico coasts have been previously associated with the wet phases, while negative anomalies have been associated with the dry phases in boreal summer (e.g. Barrett and Esquivel, 2013; PM19). Moreover, the VIMF patterns during the wet phases generally favour convective precipitation processes while conditions during the dry phases do not
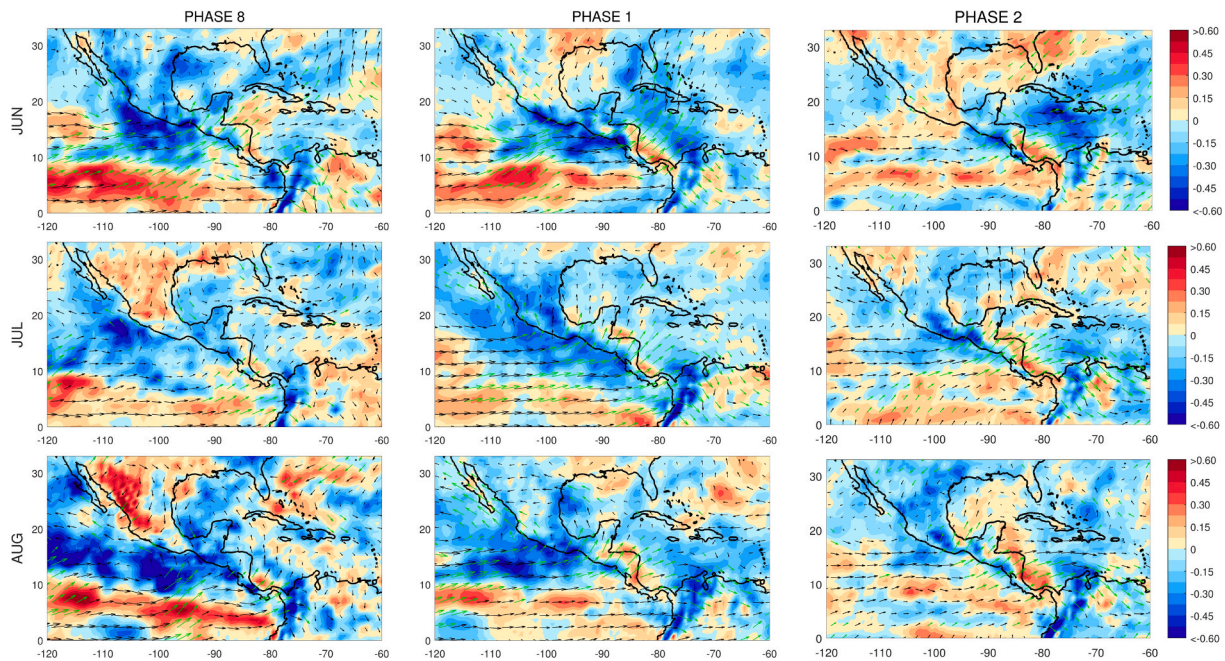
Fig. 8. Anomaly composites of the vertically integrated moisture flux (vectors, kg m^{-1} s^{-1}) and of the associated divergence (shaded, kg m^{-2} s^{-1}) binned by MJO wet phases (8, 1, 2) from June to August (the months when the MSD minimum can occur in Mexico according to PM19). The statistically significant anomalies at the 95% confidence level are indicated with green vectors.
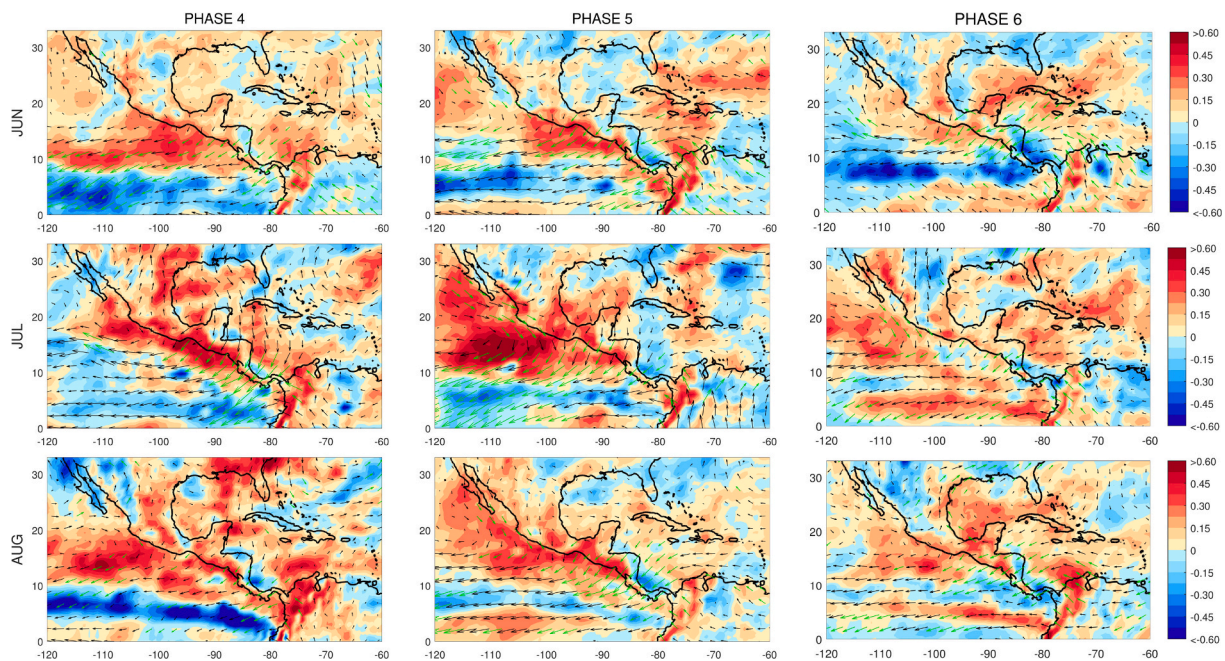

Fig. 9. As in Fig. 8, but for MJO dry phases (4, 5, 6).

(Figs. 8 and 9). Under the influence of wet phases, negative anomalies of the divergence of the VIMF are observed over the MSD region, indicating moisture flux convergence (Fig. 8). The VIMF indicates anomalous west-southwesterly moisture flux into the NETP and southern Mexico and, depending on the month, either a northwesterly or southwesterly flux into the Yucatan Peninsula (Fig. 8). The inverse pattern is observed under the influence of dry phases (Fig. 9). These VIMF patterns (Figs. 8 and 9) generally agree with the low-level wind anomalies induced by the MJO over the NETP and the Gulf of Mexico identified in previous studies (e.g. Maloney and Hartmann, 2000a, 2000b; Maloney and Esbensen, 2003, 2007; Lorenz and Hartmann, 2006; PM19).

The MSD region in Mexico is observed as a weaker moisture sink during the MJO dry phases, supported by negative anomalies of $|$ $(E - P)_{3-7} < 0$ $|$ (Fig. 7). This relationship could be caused by the strengthening of the CLLJ that occurs under the influence of these phases (e.g. Martin and Schumacher, 2011a).The anomalous east-northeasterly flow over the NETP and the Caribbean basin induced by the MJO during its dry phases intensifies the easterly flow of the CLLJ. A stronger CLLJ transports moisture from the Caribbean basin much farther west, away from Mexico and directly into the ITCZ in the NETP. Thus, the intensification of the CLLJ reinforces the westward shift of the moisture sink region in July and August (the MSD months) and reduces the moisture available to precipitate over Mexico. The strengthening of

the CLLJ during the MJO dry phases favours then an inhibition of rainfall over the MSD region in Mexico, where an increase of evaporation (Fig. 7) and moisture flux divergence (Fig. 9) is observed. Therefore, the MJO dry phases favour an atmospheric circulation pattern that inhibits precipitation over the MSD region in Mexico associated with moisture from the CLLJ core (Fig. 7).

In contrast, the anomalous west-southwesterly flow over the NETP, Mesoamerican, and Caribbean regions associated with the MJO wet phases interacts with the easterly flow of the CLLJ, weakening it and generating an anomalous moisture convergence over the MSD region in Mexico (see Figs. 6 and 8). A weaker CLLJ leads to an enhancement of moisture from the Caribbean over Mexico, making it a stronger moisture sink (see in Fig. 6 the positive anomalies of $|(E - P)_{3-7} < 0|$ over the MSD region in Mexico). In others words, under the influence of a weaker low-level easterly flow, the moisture transported by the CLLJ is not capable to reach the NETP and is thus available to precipitate over Mexico. This precipitation is further favoured by the stronger instability present during the MJO wet phases (e.g. Maloney and Hartmann, 2000a; Maloney and Esbensen, 2003, 2007; Barlow and Salstein, 2006; Lorenz and Hartmann, 2006; PM19). Note that the MJO dry phases (and not the wet phases) are the most frequent during the MSD months (i.e., July and August) in Mexico (PM19). The greater moisture contribution from the CLLJ core is obtained over southern Mexico, mainly in July during phase 2 and in August during phase 1 (Fig. 6). The MJO wet phases therefore enhance an atmospheric circulation pattern that favours precipitation over the MSD region associated with moisture from the CLLJ core (Fig. 6).

The NETP was found to be a weaker moisture sink under the influence of MJO phases 1 and 2 (see in Fig. 6 the negative anomalies of $|(E - P)_{3-7} < 0|$ over the NETP), despite the negative climatological values of $(E - P)_{1-10}$ observed in this region (see Fig. 3). In addition, the Intra-Americas Sea was generally found to be a stronger moisture sink during these MJO phases, despite the fact that the climatological pattern of $(E - P)_{1-10}$ does not show a moisture contribution from the CLLJ core therein (except over the Caribbean coast of the southern half of Central America) (see Figs. 3 and 6). Therefore, as mentioned above, the west-southwesterly anomalies of the VIMF imposed by the MJO wet phases maintain the moisture from the CLLJ core over the Intra-Americas Sea and the Mesoamerican region, which prevents its

transport to the NETP (see Fig. 8). Hence, the strong positive rainfall anomalies that are obtained over the NETP in September under the influence of the MJO wet phases (see Fig. 2 in PM19) are associated with precipitation in the MJO convective envelope itself, and not a teleconnection pattern.

The results shown thus far indicate that MJO influences the summer rainfall pattern in the MSD region in Mexico by modulating the moisture transport mechanism from the Caribbean to Mexico. MJO-related low-level wind anomalies weaken or strengthen the CLLJ. This variability in the intensity of the CLLJ influences the moisture transport towards Mexico, making the MSD region a stronger moisture sink in MJO wet phases and a weaker moisture sink in MJO dry phases.

3.4. Influence of the MJO on the moisture transport from the NETP

No relationship was previously found between the moisture transport from the CLLJ core and the occurrence of the MSD in August over southwestern Mexico (see Section 3.2). Additionally, the NETP was not identified before as a climatological moisture source for the MSD region (see Section 3.1). Therefore, one last analysis was performed for the southwest region in order to gain insights into the variability of its bimodal distribution of rainfall in association with the MJO. For this, the monthly anomaly composites of $(E - P)_{1-10} > 0$ for the southwest of Mexico obtained by backward in time trajectories and according to different MJO phases for the summer months were analysed. Only positive values of $(E - P)_{1-10}$ were used to calculate these anomalies in order to analyse how the MJO modulates the moisture source regions for southwestern Mexico. The results indicated that, while an area with positive anomalies within the NETP emerges as a moisture source for the southwestern region in July (when the first rainfall maximum occurs in this region according to Perdigón-Morales et al., 2018) and under the influence of MJO phases 1 and 2, in August (when the MSD occurs in this region), this is not observed (not shown). Based on these results, the squared area marked in the top panels of Fig. 10 was defined to follow the air particles forwards in time.

The air parcels advected from the NETP typically arrive in southwestern Mexico one day later (see Fig. S1 in Supplementary Material). In this case, the moisture contribution to precipitation over the southwest region is not negligible in the sixth day, so a minimal average
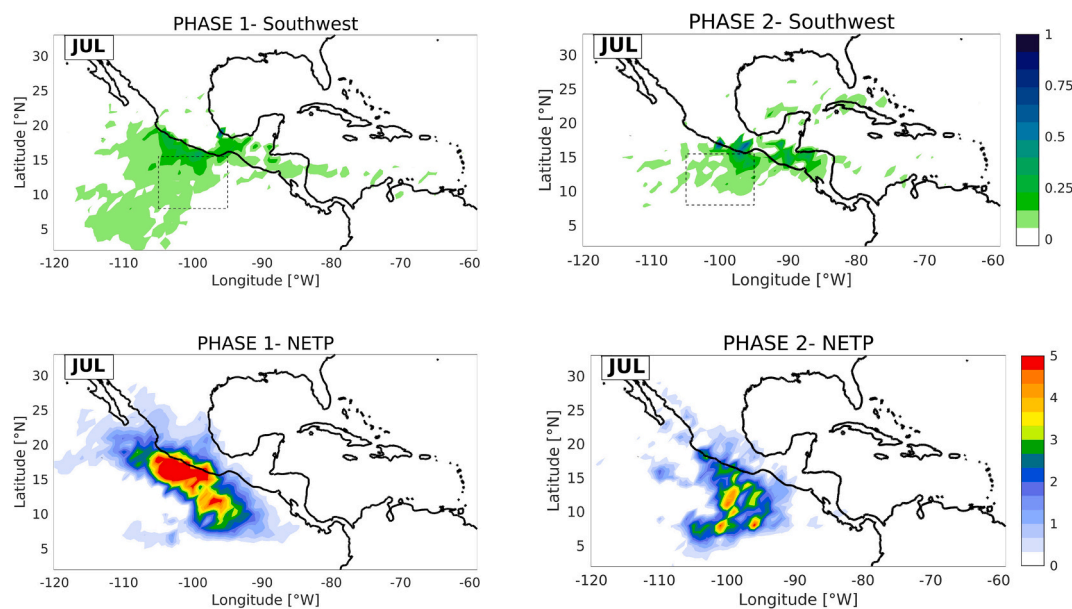

Fig. 10. Positive anomalies of $(E - P) > 0$ values (mm day^{-1}) integrated backwards over 1–6 days from the southwestern region of Mexico for MJO phases 1 and 2 in July (top panels) (Note: shaded areas represent evaporative moisture sources). Positive anomalies of $|(E - P) < 0|$ values (mm day^{-1}) integrated forwards over 1–6 days from the NETP region for MJO phases 1 and 2 in July (bottom panels) (Note: shaded areas represent moisture sinks).

window was taken to be 1–6 days for the temporal range of the trajectories. Hence, the water vapour flux integrated over 1–6 days after air masses leave the NETP region was computed for July for the period 1979–2017, and the anomalies of the absolute values of $(E - P)_{1-6} < 0$, i.e. $| (E - P)_{1-6} < 0 |$, binned by MJO phases 1 and 2 were then calculated. Similar as before (see section 3.3), only negative values of $(E - P)_{1-6}$ were used to calculate the anomalies for the purpose of examining the influence of the MJO on the moisture sink regions over Mexico associated with the moisture from the NETP region. The average window of 1–6 days was used to recalculate the monthly anomaly composites of the water vapour balance for the southwest of Mexico obtained by backward in time trajectories and according to the MJO phases; the results for July and MJO phases 1 and 2 are shown in Fig. 10 (top panels).

The southwestern region of Mexico and its Pacific Ocean coasts were found to be a stronger moisture sink related to the NETP region under the influence of the MJO phases 1 and 2 in July (Fig. 10, bottom panels). PM19 found that phases 1 and 2 are the most frequent during the first rainfall peak in southwestern Mexico and concluded that the MJO influences the bimodal pattern of precipitation in this region by increasing rainfall amounts during this first rainfall peak. However, a physical mechanism was not provided in their study. The results of this section, jointly with those obtained by PM19, suggest an influence of the MJO phases 1 and 2 on the bimodal precipitation pattern in southwestern Mexico by increasing the moisture supply from the NETP in July, the month of the first rainfall peak in this region. Even more research is needed to improve knowledge about the role of the MJO in modulating the seasonal rainfall cycle in this region.

4. Summary and conclusions

The MSD in Mexico is modulated by changes in the convective and circulation patterns associated with the eastward propagation of the MJO (PM19). Until this present study, however, a physical mechanism linking the MJO to the MSD in Mexico remained unclear. In this work, our understanding of how the MJO modulates the MSD in Mexico is improved. For this purpose, the Lagrangian particle dispersion model FLEXPART was used to analyse the transport of water vapour towards the MSD region in Mexico and the role that the MJO plays in it.

Four representative subregions of different types of MSD in Mexico were chosen for the analyses: the southwest, south, northeast, and the Yucatan Peninsula (see Fig. 1). The Caribbean Sea was identified as an important moisture source for the south, northeast, and Yucatan, but not for southwestern Mexico. The region of maximum moisture gain over the Caribbean area generally coincides with the CLLJ core region, specially for the region of southern Mexico and from June to September, in agreement with previous studies (e.g. Wang, 2007; Durán-Quesada et al., 2010). This evaporative source also shows a clear seasonal variability during the summer, which is closely related to the seasonal variability of the CLLJ. More importantly, the results presented here show that the CLLJ favours the bimodal precipitation patterns identified in these MSD subregions of Mexico, with the exception of the southwest. The CLLJ dynamics favour drier conditions during the MSD minimum months in most of Mexico, carrying less moisture towards it. During July and August, when the CLLJ strengthens and reaches a maximum (Wang, 2007), the moisture sink region over Mexico presents a remarkable westward shift compared to the previous two months, favouring thus the occurrence of the MSD. In September and October, when the CLLJ weakens (Wang, 2007), the moisture contribution from the CLLJ core to precipitation over Mexico increases again over the entire MSD region. The results of this analysis are in agreement with previous studies regarding the importance of the temporal variability of the CLLJ, and its associated dynamical processes, as crucial to explain the MSD in the tropical Americas (e.g. Wang, 2007; Cook and Vizy, 2010; Martin and Schumacher, 2011a; Herrera et al., 2015; Hidalgo et al., 2015).

The MJO modulates the water vapour flux transported by the CLLJ towards the MSD region in Mexico. The MJO wet phases (8, 1, and 2) favour an increase in the moisture contribution to the MSD region coming from the CLLJ, while the MJO dry phases (4, 5, and 6) favour a decrease of moisture from the CLLJ region. The intensification of the CLLJ under the influence of the MJO dry phases favours an increase of evaporation and moisture flux divergence over the MSD region and, thereby, the aforementioned westward shift of the moisture sink region over Mexico is further reinforced. The MJO dry phases therefore favour an atmospheric circulation pattern that inhibits precipitation associated with the moisture source of the CLLJ core over the MSD region in Mexico. In addition, the MJO dry phases are the most frequent during the MSD minimum in Mexico (PM19). Thus, the MJO dry phases influence the intraseasonal pattern of rainfall inhibiting the convection and precipitation during the MSD minimum by decreasing the moisture contribution from the CLLJ core to precipitation over the MSD region. However, in a given year, the MJO could influence in the opposite sense, that is, the wet phases could weaken the processes that inhibit precipitation during the MSD minimum (PM19). As the CLLJ weakens under the influence of the MJO wet phases, the moisture sink region over Mexico does not present the westward shift. Consequently, there is
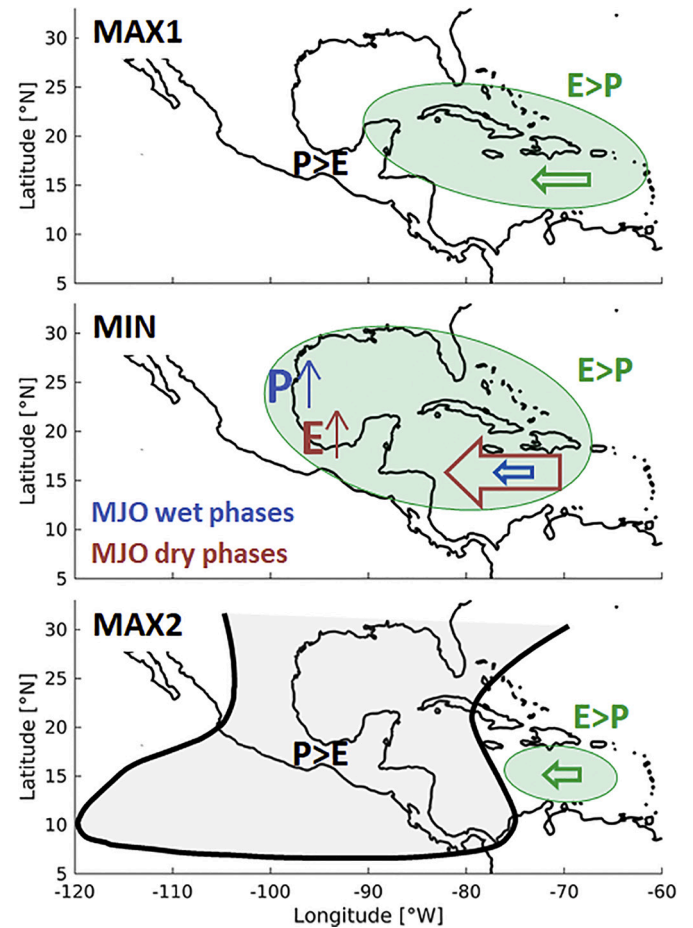

Fig. 11. Schematic diagram of the physical mechanism linking the MJO to the MSD over Mexico based on a combined MJO-CLLJ action. Green and black colors indicate climatology conditions. Green ellipses indicate the area where evaporation exceeds precipitation $(E > P)$; conversely, the black curve encloses the area where precipitation exceeds evaporation $(P > E)$. The anomalies associated with the MJO during the MSD minimum are indicated, in red representing the influence of its dry phases (strengthening of average conditions, negative precipitation anomalies over the MSD region), and in blue representing the influence of its wet phases (weakening of average conditions, positive precipitation anomalies over the MSD region). The length of the thick arrows indicates the anomalies of the CLLJ associated with the MJO.

an increase of the moisture flux convergence and the moisture contribution from the CLLJ core to precipitation in Mexico during the MSD minimum.

The CLLJ was not found to influence the occurrence of the MSD in the southwestern region. However, the results suggest that the MJO influences the first rainfall peak of the season in the southwestern region of Mexico as a result of an increase in moisture supply from the NETP under phases 1 and 2 in July. Although PM19 showed that the MJO wet phases favour convection and precipitation during the first rainfall peak in southwestern Mexico (see Fig. 10 in PM19), a physical mechanism linking the MJO and this increase in rainfall was not provided in their study. Furthermore, the present work explains part of the spatiotemporal variability of the MSD by highlighting, for example, the behaviour of the MSD over the Yucatan Peninsula, where the MSD occurs in July. On one hand, greater evaporation in July (with respect to June and August) is clearly observed over this region (Figs. 3 and 4). Moreover, strong positive anomalies are noted in August under the influence of MJO phase 8, which in turn is the most frequent phase during the second peak of precipitation in the Yucatan Peninsula (PM19).

In summary, the MJO amplifies the bimodal rainfall pattern over most of the Mexican MSD region by modulating the moisture amount transported by the CLLJ. This proposed mechanism is outlined in Fig. 11. Critical in the mechanism proposed here are the strong seasonality in moisture advected from the Caribbean basin to the MSD region, and the influence of the MJO on both the moisture transported by the CLLJ and the MSD in Mexico. Finally, a subseasonal prediction system could be improved from consideration of the seasonal evolution of the MJO and of its effect over regional circulation mechanisms (e.g. Li et al., 2013; Serra et al., 2014; Liu et al., 2020). These mechanisms are strongly associated with seasonal rainfall patterns in regions around the globe. Hence, this study provides a potential source of predictability of the seasonal rainfall cycle in the MSD region in Mexico, since it shows new evidence of the seasonal evolution of the MJO teleconnection over the Western Hemisphere.

Supplementary data to this article can be found online at https://doi.org/10.1016/j.atmosres.2020.105243.

Authorship contributions

Conception and design of study: J. Perdigón-Morales, P. Ordoñez, R. Nieto, and L. Gimeno.

Acquisition of data: J. Perdigón-Morales, R. Nieto, and L. Gimeno.

Analysis and/or interpretation of data: J. Perdigón-Morales, R. Romero-Centeno, P. Ordoñez, R. Nieto, L. Gimeno, and B. Barrett.

Drafting the manuscript: J. Perdigón-Morales.

Revising the manuscript critically for important intellectual content: J. Perdigón-Morales, R. Romero-Centeno, P. Ordoñez, R. Nieto, L. Gimeno, and B. Barrett.

Approval of the version of the manuscript to be published: J. Perdigón-Morales, R. Romero-Centeno, P. Ordoñez, R. Nieto, L. Gimeno, and B. Barrett.

Declaration of Competing Interest

The authors declare that they have no conflict of interest.

References

Algarra, I., Eiras-Barca, J., Miguez-Macho, G., Nieto, R., Gimeno, L., 2019. On the assessment of the moisture transport by the Great Plains low-level jet. Earth Syst. Dyn. 10 (1). https://doi.org/10.5194/esd-10-107-2019.

Amador, J.A., 1998. A climatic feature of the tropical Americas: the trade wind easterly jet. Top Meteor Oceanogr. 5 (2), 1–13.

Amador, J.A., Magaña, V.O., Pérez, J.B., 2000. The low level jet and convective activity in the Caribbean. Preprints. In: 24th Conference in Hurricanes and Tropical Meteorology. American Meteorological Society. 1, pp. 114–115.

Amador, J.A., Alfaro, E.J., Lizano, O.G., Magaña, V.O., 2006. Atmospheric forcing of the eastern tropical Pacific: a review. Prog. Oceanogr. 69, 101–142. https://doi.org/10.1016/j.pocean.2006.03.007.

Barlow, M., Salstein, D., 2006. Summertime influence of the Madden–Julian oscillation on daily rainfall over Mexico and Central America. Geophys. Res. Lett. 33, L21708. https://doi.org/10.1029/2006GL027738.

Barrett, B.S., Esquivel, M.I., 2013. Variability of precipitation and temperature in Guanajuato. Mexico. Atmósfera. 26, 521–536. https://doi.org/10.1016/S0187-6236(13)71093-2.

Barrett, B.S., Leslie, L.M., 2009. Links between tropical cyclone activity and Madden–Julian oscillation phase in the North Atlantic and Northeast Pacific basins. Mon. Weather Rev. 137 (2), 727–744. https://doi.org/10.1175/2008MWR2602.1.

Bosilovich, M.G., Sud, Y.C., Schubert, S.D., Walker, G.K., 2003. Numerical simulation of the large-scale north American monsoon water sources. J. Geophys. Res. 108, 8614. https://doi.org/10.1029/2002JD003095.

Brubaker, K.L., Entekhabi, D., Eagleson, P.S., 1993. Estimation of continental precipitation recycling. J. Clim. 6, 1077–1089. https://doi.org/10.1175/1520-0442(1993)006<1077:EOCPR>2.0.CO;2.

Cook, K.H., Vizy, E.K., 2010. Hydrodynamics of the Caribbean low-level jet and its relationship to precipitation. J. Clim. 23 (6), 1477–1494. https://doi.org/10.1175/2009JCLI3210.1.

Crosbie, E., Serra, Y., 2014. Intraseasonal modulation of synoptic-scale disturbances and tropical cyclone genesis in the eastern North Pacific. J. Clim. 27 (15), 5724–5745. https://doi.org/10.1175/JCLI-D-13-00399.1.

Curtis, S., 2002. Interannual variability of the bimodal distribution of summertime rainfall over Central America and tropical storm activity in the far-eastern Pacific. Clim. Res. 22 (2), 141–146. https://doi.org/10.3354/cr022141.

Curtis, S., Gamble, D.W., 2016. The boreal winter Madden–Julian Oscillation's influence on summertime precipitation in the greater Caribbean. J. Geophys. Res. Atmos. 121, 7592–7605. https://doi.org/10.1002/2016JD025031.

Dee, D.P., et al., 2011. The ERA-Interim reanalysis: Configuration and performance of the data assimilation system. Q. J. R. Meteorol. Soc. 137, 553–597. https://doi.org/10.1002/qj.828.

Durán-Quesada, A.M., Gimeno, L., Amador, J.A., Nieto, R., 2010. Moisture sources for Central America: Identification of moisture sources using a Lagrangian analysis technique. J. Geophys. Res. Atmos. 115 (D5). https://doi.org/10.1029/2009JD012455.

Durán-Quesada, A.M., Reboita, M., Gimeno, L., 2012. Precipitation in tropical America and the associated sources of moisture: a short review. Hydrol. Sci. J. 57 (4), 612–624. https://doi.org/10.1080/02626667.2012.673723.

Durán-Quesada, A.M., Gimeno, L., Amador, J.A., 2017. Role of moisture transport for central American precipitation. Earth Syst. Dyn. 8, 147–161. https://doi.org/10.5194/esd-8-147-2017.

Efron, B., Tibshirani, R.J., 1994. An Introduction to the Bootstrap. CRC Press 430pp.

Gamble, D.W., Curtis, S., 2008. Caribbean precipitation: review, model and prospect. Prog. Phys. Geogr. 32 (3), 265–276. https://doi.org/10.1177/0309133308096027.

Gamble, D.W., Parnell, D.B., Curtis, S., 2008. Spatial variability of the Caribbean midsummer drought and relation to North Atlantic high circulation. Int. J. Climatol. 28, 343–350. https://doi.org/10.1002/joc.1600.

García-Martínez, I.M., Bollasina, M.A., 2020. Sub-monthly evolution of the Caribbean Low-Level Jet and its relationship with regional precipitation and atmospheric circulation. Clim. Dyn. 1–18. https://doi.org/10.1007/s00382-020-05237.

Giannini, A., Kushnir, Y., Cane, M.A., 2000. Interannual variability of Caribbean rainfall,

ENSO, and the Atlantic Ocean. J. Clim. 13, 297–311. https://doi.org/10.1175/1520-0442(2000)013<0297:IVOCRE>2.0.CO;2.

Gimeno, L., Stohl, A., Trigo, R.M., Dominguez, F., Yoshimura, K., Yu, L., Drumond, A., Durán-Quesada, A.M., Nieto, R., 2012. Oceanic and terrestrial sources of continental precipitation. Rev. Geophys. 50, RG4003. https://doi.org/10.1029/2012RG000389.

Gimeno, L., Nieto, R., Drumond, A., Castillo, R., Trigo, R., 2013. Influence of the intensification of the major oceanic moisture sources on continental precipitation. Geophys. Res. Lett. 40 (7), 1443–1450. https://doi.org/10.1002/grl.50338.

Gimeno, L., Vázquez, M., Eiras-Barca, J., Sorí, R., Stojanovic, M., Algarra, I., Nieto, R., Ramos, A.M., Durán-Quesada, A.M., Dominguez, F., 2020. Recent progress on the sources of continental precipitation as revealed by moisture transport analysis. Earth Sci. Rev. 201, 103070. https://doi.org/10.1016/j.earscirev.2019.103070.

Hendon, H.H., Salby, M.L., 1994. The life cycle of the Madden–Julian oscillation. J. Atmos. Sci. 51, 2225–2237. https://doi.org/10.1175/1520-0469(1994)051<2225:TLCOTM>2.0.CO;2.

Herrera, E., Magaña, V., Caetano, E., 2015. Air–sea interactions and dynamical processes associated with the midsummer drought. Int. J. Climatol. 35, 1569–1578. https://doi.org/10.1002/joc.4077.

Hidalgo, H.G., Durán-Quesada, A.M., Amador, J.A., Alfaro, E.J., 2015. The Caribbean low-level jet, the inter-tropical convergence zone and precipitation patterns in the intra-Americas sea: a proposed dynamical mechanism. Geografiska Annaler: Series A Physical Geography. 97 (1), 41–59. https://doi.org/10.1111/geoa.12085.

Higgins, R., Shi, W., 2001. Intercomparison of the principal modes of interannual and intraseasonal variability of the north American monsoon system. J. Clim. 14 (3), 403–417. https://doi.org/10.1175/1520-0442(2001)014<0403:IOTPMO>2.0.CO;2.

Jones, C., Carvalho, L.M.V., 2011. Stochastic simulations of the Madden–Julian oscillation activity. Clim. Dyn. 36, 229–246. https://doi.org/10.1007/s00382-009-0660-2.

Karnauskas, K.B., Seager, R., Giannini, A, Busalacchi, A.J., 2013. A simple mechanism for the climatological midsummer drought along the Pacific coast of Central America. Atmósfera. 26, 261–281. https://doi.org/10.1016/S0187-6236(13)71075-0.

Klotzbach, P.J., 2010. On the Madden–Julian oscillation–Atlantic hurricane relationship. J. Clim. 23 (2), 282–293. https://doi.org/10.1175/2009JCLI2978.1.

Li, K., Yu, W., Li, T., Murty, V.S.N., Khokiattiwong, S., Adi, T.R., Budi, S., 2013. Structures and mechanisms of the first-branch northward-propagating intraseasonal oscillation over the tropical Indian Ocean. Clim. Dyn. 40 (7–8), 1707–1720. https://doi.org/10.1007/s00382-012-1492-z.

Liu, F., Ouyang, Y., Wang, B., Yang, J., Ling, J., Hsu, P.C., 2020. Seasonal evolution of the intraseasonal variability of China summer precipitation. Clim. Dyn. 1–15. https://doi.org/10.1007/s00382-020-05251-0.

Lorenz, D.J., Hartmann, D.L., 2006. The effect of the MJO on the north American monsoon. J. Clim. 19 (3), 333–343. https://doi.org/10.1175/JCLI3684.1.

Madden, R.A., Julian, P.R., 1994. Observations of the 40–50 day tropical oscillation—a review. Mon. Weather Rev. 122, 814–837. https://doi.org/10.1175/1520-0493(1994)122<0814:OOTDTO>2.0.CO;2.

Magaña, V., Caetano, E., 2005. Temporal evolution of summer convective activity over the Americas warm pools. Geophys. Res. Lett. 32, L02803. https://doi.org/10.1029/2004GL021033.

Magaña, V., Amador, J.A., Medina, S., 1999. The midsummer drought over Mexico and Central America. J. Clim. 12, 1577–1588. https://doi.org/10.1175/1520-0442(1999)012<1577:TMDOMA>2.0.CO;2.

Maldonado, T., Rutgersson, A., Alfaro, E., Amador, J., Claremar, B., 2016. Interannual variability of the midsummer drought in Central America and the connection with sea surface temperatures. Adv. Geosci. 42, 35–50. https://doi.org/10.5194/adgeo-42-35-2016.

Maloney, E.D., Esbensen, S.K., 2003. The amplification of East Pacific Madden–Julian oscillation convection and wind anomalies during June–November. J. Clim. 16 (21), 3482–3497. https://doi.org/10.1175/1520-0442(2003)016<3482:TAOEPM>2.0.CO;2.

Maloney, E.D., Esbensen, S.K., 2007. Satellite and buoy observations of boreal summer intraseasonal variability in the tropical Northeast Pacific. Mon. Weather Rev. 135 (1), 3–19. https://doi.org/10.1175/MWR3271.1.

Maloney, E.D., Hartmann, D.L., 2000a. Modulation of eastern North Pacific hurricanes by the Madden–Julian oscillation. J. Clim. 13, 1451–1460. https://doi.org/10.1175/1520-0442(2000)013<1451:MOENPH>2.0.CO;2.

Maloney, E.D., Hartmann, D.L., 2000b. Modulation of hurricane activity in the Gulf of Mexico by the Madden–Julian oscillation. Science. 287, 2002–2004. https://doi.org/10.1126/science.287.5460.2002.

Maloney, E.D., Kiehl, J.T., 2002. MJO-related SST variations over the tropical eastern Pacific during Northern Hemisphere summer. J. Clim. 15 (6), 675–689. https://doi.org/10.1175/1520-0442(2002)015<0675:MRSVOT>2.0.CO;2.

Maloney, E.D., Chelton, D.B., Esbensen, S.K., 2008. Subseasonal SST variability in the tropical eastern North Pacific during boreal summer. J. Clim. 21 (17), 4149–4167. https://doi.org/10.1175/2007JCLI1856.1.

Mapes, B.E., Liu, P., Buenning, N., 2005. Indian monsoon onset and the Americas midsummer drought: Out-of-equilibrium responses to smooth seasonal forcing. J. Clim. 18, 1109–1115. https://doi.org/10.1175/JCLI-3310.1.

Martin, E.R., Schumacher, C., 2011a. Modulation of Caribbean precipitation by the Madden–Julian oscillation. J. Clim. 24, 813–824. https://doi.org/10.1175/2010JCLI3773.1.

Martin, E.R., Schumacher, C., 2011b. The Caribbean low-level jet and its relationship with precipitation in IPCC AR4 models. J. Clim. 24 (22), 5935–5950. https://doi.org/10.1175/JCLI-D-11-00134.1.

Mestas-Nuñez, A.M., Enfield, D.B., Zhang, C., 2007. Water vapor fluxes over the Intra-Americas Sea: Seasonal and interannual variability and associations with rainfall. J. Clim. 20 (9), 1910–1922. https://doi.org/10.1175/JCLI4096.1.

Mitchell, D.L., Ivanova, D., Rabin, R., Brown, T.J., Redmond, K., 2002. Gulf of California Sea surface temperatures and the north American monsoon: Mechanistic implications from observations. J. Clim. 15, 2261–2281. https://doi.org/10.1175/1520-0442(2002)015<2261:GOCSST>2.0.CO;2.

Muñoz, E., Busalacchi, A.J., Nigam, S., Ruiz-Barradas, A., 2008. Winter and summer structure of the Caribbean low-level jet. J. Clim. 21 (6), 1260–1276. https://doi.org/10.1175/2007JCLI1855.1.

Nieto, R., Gimeno, L., 2019. A database of optimal integration times for Lagrangian studies of atmospheric moisture sources and sinks. Sci. Data. 6 (1), 1–10. https://www.nature.com/articles/s41597-019-0068-8.

Nieto, R., Castillo, R., Drumond, A., Gimeno, L., 2014. A catalog of moisture sources for continental climatic regions. Water Resourc. Res. 50, 5322–5328. https://doi.org/10.1002/2013WR013901.

Ordonez, P., Ribera, P., Gallego, D., Pena-Ortiz, C., 2013. Influence of Madden-Julian Oscillation on water budget transported by the Somali low-level jet and the associated Indian summer monsoon rainfall. Water Resourc. Res. 49 (10), 6474–6485. https://doi.org/10.1002/wrcr.20515.

Ordoñez, P., Nieto, R., Gimeno, L., Ribera, P., Gallego, D., Ochoa-Moya, C.A., Quintanar, A.I., 2019. Climatological moisture sources for the Western north American Monsoon through a Lagrangian approach: their influence on precipitation intensity. Earth Syst. Dyn. 10 (1), 59–72. https://doi.org/10.5194/esd-10-59-2019.

Perdigón-Morales, J., Romero-Centeno, R., Ordóñez, P., Barrett, B.S., 2018. The midsummer drought in Mexico: Perspectives on duration and intensity from the CHIRPS precipitation database. Int. J. Climatol. 38, 2174–2186. https://doi.org/10.1002/joc.5322.

Perdigón-Morales, J., Romero-Centeno, R., Barrett, B.S., Ordóñez, P., 2019. Intraseasonal variability of summer precipitation in Mexico: MJO influence on the midsummer drought. J. Clim. 32, 2313–2327. https://doi.org/10.1175/JCLI-D-18-0425.1.

Ramos, A.M., Nieto, R., Tomé, R., Gimeno, L., Trigo, R.M., Liberato, M.L., Lavers, D.A., 2016. Atmospheric rivers moisture sources from a Lagrangian perspective. Earth Syst. Dyn. 7 (2), 371–384. https://d-nb.info/1142400778/34.

Romero-Centeno, R., Zavala-Hidalgo, J., Raga, G.B., 2007. Mid-summer gap winds and low-level circulation over the eastern tropical Pacific. J. Clim. 20, 3768–3784. https://doi.org/10.1175/JCLI4220.1.

Serra, Y.L., Jiang, X., Tian, B., Amador-Astua, J., Maloney, E.D., Kiladis, G.N., 2014. Tropical intraseasonal modes of the atmosphere. Annu. Rev. Environ. Resour. 39, 189–215. https://doi.org/10.1146/annurev-environ-020413-134219.

Small, R.J., Szoeke, S.P., Xie, S.P., 2007. The central American midsummer drought: Regional aspects and large-scale forcing. J. Clim. 20, 4853–4873. https://doi.org/10.1175/JCLI4261.1.

Stohl, A., James, P., 2004. A Lagrangian analysis of the atmospheric branch of the global water cycle. Part 1: Method description, validation, and demonstration for the August 2002 flooding in Central Europe. J. Hydrometeorol. 5, 656–678. https://doi.org/10.1175/1525-7541(2004)005<0656:ALAOTA>2.0.CO;2.

Stohl, A., James, P., 2005. A Lagrangian analysis of the atmospheric branch of the global water cycle. Part 2: Earth's river catchments, ocean basins, and moisture transports between them. J. Hydrometeorol. 6, 961–984. https://doi.org/10.1175/JHM470.1.

Stohl, A., Wotawa, G., Seibert, P., Kromp-Kolb, H., 1995. Interpolation errors in wind fields as a function of spatial and temporal resolution and their impact on different types of kinematic trajectories. J. Appl. Meteorol. 34, 2149–2165. https://doi.org/10.1175/1520-0450(1995)034<2149:IEIWFA>2.0.CO;2.

Trenberth, K.E., 1999. Atmospheric moisture recycling: role of advection and local evaporation. J. Clim. 12, 1368–1381. https://doi.org/10.1175/1520-0442(1999)012<1368:AMRROA>2.0.CO;2.

Van Der Ent, R.J., Tuinenburg, O.A., 2017. The residence time of water in the atmosphere revisited. Hydrol. Earth Syst. Sci. 21 (2), 779–790. https://dspace.library.uu.nl/bitstream/handle/1874/347558/Residence.pdf?sequence=1.

Wang, C., 2007. Variability of the Caribbean low-level jet and its relations to climate. Clim. Dyn. 29 (4), 411–422. https://doi.org/10.1007/s00382-007-0243-z.

Wheeler, M.C., Hendon, H.H., 2004. An all-season real-time multivariate MJO index: development of an index for monitoring and prediction. Mon. Weather Rev. 132, 1917–1932. https://doi.org/10.1175/1520-0493(2004)132<1917:AARMMI>2.0.CO;2.

Whyte, F.S., Taylor, M.A., Stephenson, T.S., Campbell, J.D., 2008. Features of the Caribbean low level jet. Int. J. Climatol. 28 (1), 119–128. https://doi.org/10.1002/joc.1510.

Zhao, Z., Oliver, E.C., Ballestero, D., Vargas-Hernandez, J.M., Holbrook, N.J., 2019. Influence of the Madden–Julian oscillation on Costa Rican mid-summer drought timing. Int. J. Climatol. 39 (1), 292–301. https://doi.org/10.1002/joc.5806.

Zhou, S., L'Heureux, M., Weaver, S., Kumar, A., 2012. A composite study of the MJO influence on the surface air temperature and precipitation over the continental United States. Clim. Dyn. 38, 1459–1471. https://doi.org/10.1007/s00382-011-1001-9.